Satellite Star Tracker Breadboard with Space Debris Detection Capability for LEO

Satellite Star Tracker Breadboard with Space Debris Detection Capability for LEO

Joel Filho[1,2], Paulo Gordo[2], Nuno Peixinho[1], Ricardo Gafeira[1], Rui Melicio[3,4] and André Silva[5]

[1]Instituto de Astrofísica e Ciências do Espaço, Departamento de Fisíca, Universidade de Coimbra, Coimbra, Portugal
[2]CENTRA, Faculdade de Ciências, Universidade de Lisboa, Lisboa, Portugal
[3]IDMEC, Instituto Superior Técnico, Universidade de Lisboa, Lisboa, Portugal
[4]ICT, Universidade de Évora, Évora, Portugal
[5]AEROG, Universidade da Beira Interior, Covilhã, Portugal

Abstract. This paper evaluates the possibility of having a star tracker device running space debris algorithms. A simple star tracker breadboard was developed to evaluate the possibility of having a device running both stellar identification and space debris algorithms. The breadboard was built with commercial off-the-shelf components, representing the current star tracker resolution and field of view. A star tracker device and space debris algorithms were implemented and tested, respectively: Tetra and ASTRiDE. The device concept was tested by taking pictures of the night sky with satellite streaks. Seeking to overcome such limitations, a dual-purpose star tracker with stars detection and optical debris detection capability is proposed. Star trackers are usually used in satellites for attitude determination and therefore have a vast potential to be a major tool for space debris detection. The rapid increase of space debris poses a risk to space activities, so it is vital to detect it. Ground-based radar and optical telescope techniques used for debris detection are limited by a size threshold, detecting only a tiny amount of the total, reason why evaluating the possibility of detecting them in space is of major importance.

Keywords. Satellite; Star tracker; Star identification; Space debris; Detection; LEO; Attitude control; Satellite streaks

1. Introduction

Since the beginning of space activities, there have been more than 6200 launches, placing into Earth orbit more than 13000 satellites. These space activities also lead to a huge amount of orbital debris or 'space junk' being, by definition, any human-made object, or fragments or portions of it, in orbit around the Earth that no longer serve a useful function [1-2].

Space debris is recognized by space agencies as a planetary threat [3]. Based on recent estimates, the number of orbital debris in space amounts to 139 million [4]. Such overpopulation of debris increases the chance of several events that could lead to catastrophic consequences, such as collisions, fragmentations, and uncontrolled reentries in the Earth's atmosphere [4-9]. Such a risk forced worldwide space agencies to develop a set of countermeasures to prevent and/or mitigate possible threats.

To continue to operate missions in orbit safely, the observation and tracking of debris are essential. Usually, these are done by optical and radar ground-based telescopes. These observations have a size threshold ranging from 10 cm in Low Earth orbit (LEO) to about 1 m in Geostationary Earth orbit

(GEO), resulting in more than 31000 space objects that are regularly tracked and held in a catalog by Space Surveillance Networks. However, such debris is only a tiny amount of the total. The non-traceable objects are obtained statistically from debris environmental models [10].

This paper aims to overcome such limitations by studying a different approach to debris observation: the usage of star trackers (STR)s devices, the most accurate attitude sensors available for modern spacecraft with errors typically in the order of a few arcseconds or less [11-13]. A satellite's attitude is determined by detecting stars in the star tracker's field of view (FOV). An algorithm identifies stars in the FOV using an internal catalog. Based on this information, the satellite attitude is computed [14].

Optical space debris detection consists of detecting faint and small moving objects over a fixed background of stars. Given their fast orbital velocity, space debris observation in LEO has a short pass duration and short FOV cross-time. Therefore, these moving objects appear in the image as elongated spots or broad lines, usually known as streaks [15].

This paper describes the initial activities for developing an STR breadboard that can be used for space debris detection. Developing such a device capable of extracting both the attitude of a satellite and detecting debris will be groundbreaking for space safety.

This paper has the following structure: Section 2 presents the star tracker breadboard design and implementation; Section 3 presents the star and debris detection software; Section 4 presents the experimental methods and results. Finally, Section 5 outlines the conclusions.

2. Breadboard Design and Implementation

2.1. *Breadboard Architecture*

The architecture of the breadboard consisted of the computer laptop, the *Camera interface+camera controller*; the *Image sensor*; the *Optics*; the *Temperature sensor*; the *Temperature controller*. The star tracker architecture breadboard is shown in Figure 1.

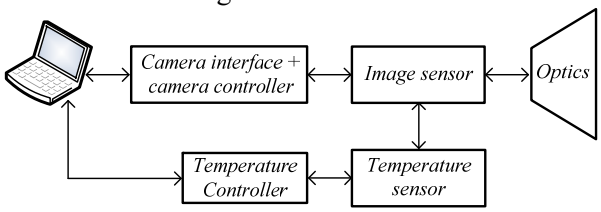

Figure 1. Architecture of the breadboard.

All components used in implementing the star tracker are commercial off-the-shelf (COTS). The selected image sensor was an Aptina MT9J001 monochromatic CMOS sensor of 10 MP. This sensor was already available at the Photonics Laboratory, Department of Physics, Faculdade de Ciências, Universidade de Lisboa, Portugal.

The breadboard's major parts were: the camera control board, image sensor, and lens (optics). The sensor is connected in an Arducam using a 30-pin ribbon cable in the secondary camera interface. The system is connected to a computer to control the camera and take images. The image sensor MT9J001 (a), the Arducam assembled on an enclosure (b), and the breadboard with the lens (c) are shown in Figure 2.

(a) (b) (c)

Figure 2. (a) Arducam and USB2 camera MT9J001; (b) sensor assembled on an enclosure; (c) breadboard with Fujian lens.

The chosen lens is a Fujian, with an f-number of 1.6 and a focal length of 35 mm. The FOV is 10.5 deg horizontally and 7.5 deg vertically, and the lens has an aperture of 22 mm.

The sensor was characterized at the Photonics Laboratory to find the camera's noise. It was calculated a readout noise (N_{RN}) of $N_{RN} = 11.97\ e^-$ and a dark current of 1.095 e−/s. Thus, the limiting magnitude of the sensor can be determined by using the noise values.

The limiting magnitude is the magnitude threshold value that the image sensor can detect. In other words, this magnitude will provide the minimum size of detectable debris. To predict the limiting magnitude, it is necessary, besides the noise values, information on the brightness of sources in specific wavebands relative to standard stars and the quantum efficiency of the sensor for different wavelengths.

The magnitude m is calculated by comparing the standard star and the object of interest given by:

$$m - m_0 = -2.5 \log\left(\frac{\Phi}{\Phi_0}\right) \tag{1}$$

In (1), m_0 and Φ_0 are the A_0 star magnitude and flux, respectively. The quantum efficiency of the sensor is provided by the spectral sensitivity curve available in the sensor datasheet. Rearranging (1) to calculate the flux for different magnitudes, taking the lens transmission coefficient, and considering that an A_0 star occupies 15 pixels in the sensor, it is possible to obtain the signal value of the sensor. With the signal and the total noise (N), the signal-to-noise ratio (SNR) in decibels is given by:

$$SNR = 10 \log\left(\frac{signal}{N}\right) \tag{2}$$

The limiting magnitude is found when SNR=1, shown in Figure 3.

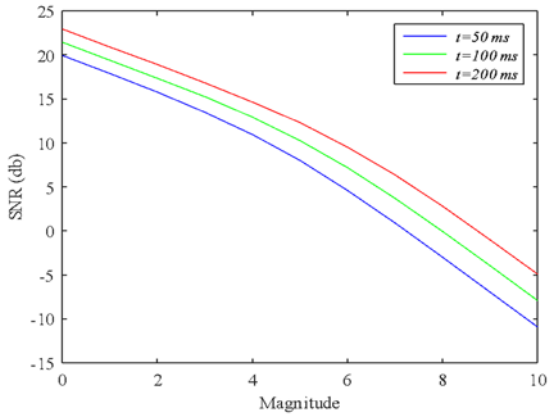

Figure 3. SNR for different magnitudes in distinct integration times.

In Figure 3, the limiting magnitude of the MT9J001 is +7 for an integration time of 50 ms, +8 for 100 ms, and +9 for 200 ms.

2.2. *Visual Magnitude of Debris*

The visual magnitude of debris relates to its capability to reflect the solar light, which depends on size, phase angle (i.e., the Sun-object-Earth angle), reflectivity, and the distance from the observer and the Sun. The debris's visual magnitude m_{debris} is given by [16]:

$$m_{debris} = M + 5\ log\left(\frac{R\,\Delta}{a^2}\right) - 2.5\ log\left[\beta F_{diff}(\phi) + (1-\beta)\,F_{spec}(\phi)\right] \tag{3}$$

In (3), M is the absolute magnitude, R is the distance from the debris to the Sun, Δ is the distance from the debris to the Earth, a is the distance between the Sun and the Earth, F is the solar phase angle function split into specular and diffuse components, being ϕ the phase angle, and β is a mixing coefficient ranging from 0 to 1. When β=0, the debris is entirely specular, while β =1 is completely diffuse. The absolute magnitude is calculated by:

$$M = m_{sun} - 2.5\ log\left(p\frac{A}{a^2}\right) \tag{4}$$

In (4), m_{sun} is the visual magnitude of the Sun, p is the geometric albedo (reflectivity), and A is the cross-section area.

Therefore, considering the latest estimation for the average reflectivity of debris is 0.175 [16] and assuming these objects are spheres, the visual magnitude can be calculated by choosing different β values at ϕ intervals and for several distances. Also, considering 17500 debris larger than 10 cm homogeneously spread over LEO orbits from 200 km to 2000 km altitude, the average distance between the debris is about 124 km. A 10 cm debris seen at 124 km will have an average magnitude of +6.0, which is within the limits of the sensor. Further, the sensor's limiting magnitude of +7 corresponds to objects of 6.2 cm seen at 124 km. Therefore, such a sensor, in space, will be able to detect debris even smaller than 10 cm.

3. Stars and Debris Detection Software

The algorithms used were Tetra and ASTRiDE. Tetra for star detection and ASTRiDE for debris detection. ASTRiDE and Tetra were chosen for being robust algorithms in detection, extremely fast, and easy to use. To compare the results provided by Tetra, Astrometry.net was used, which is a standard algorithm for attitude determination. Although, this software was not developed for star trackers.

- Tetra

Tetra [17] is an open-source algorithm developed to be used in COTS hardware that promises to use the minimum possible computation time and number of database accesses to solve the problem of the initial attitude acquisition. Tetra is a lost-in-space star identification that needs three or four stars to work. Tetra identifies four neighbor stars and divides the distance between them by the brightest star from this group of stars. This information is stored in array format, and then each array is compared to the internal catalog, stored in hash tables, to match the stars and give the attitude information.

Tetra uses the Yale bright star (BSC5) as an internal catalog. BSC5 has 9110 stars with a limiting magnitude of +6.5. However, the probability of identifying stars by the algorithm is proportional to the number of stars in the catalog. We have replaced the BSC5 with the Hipparcos catalog, which has 118218 stars and a limiting magnitude of +12.4 [18].

- ASTRiDE

ASTRiDE [19] is a fully available algorithm based on the outline shape of elongated sources that can detect fast-moving objects. To detect streaks, first, the algorithm extracts the background by calculating the background level and using its standard deviation to do the removal. After that, ASTRiDE derives the contour map for finding all the borders inside the image. Then, the algorithm uses the morphologies of each border to distinguish streaks from stars.

After the calculations, ASTRiDE generates several figures depending on the number of streak detection. It creates an image named 'all' that shows the original image with the found streaks and figures zoomed in on each linked streak. The streaks are numbered, and every individual image is denominated relative to its number. Besides that, a txt list containing information about the streaks' position, area, and perimeter in the image is also created.

4. Experimental Methods and Results

The tests were done at the Geophysical and Astronomical Observatory, Universidade de Coimbra, Portugal. The breadboard connected to the computer composes the system's drivers and controllers, processor, and software.

- *Case Study_1*

The overall system architecture, i.e., the flow chart of the breadboard operation, is shown in Figure 4.

- *Case Study_2*

The breadboard was fixed on a tripod allowing the camera's movement, and then the device was plugged into a computer to extract the images. The focus and the aperture of the lens have to be adjusted manually.

The source of streaks was satellites. It is possible to discover the position of satellites by searching on the internet. Then, the system was directed to that specific location. The exposure time was 10 s. The camera was programmed to save the images automatically until the stop button was pressed. It obtained thirteen images with a streak on them. In a few of them, the source of the streak is the same, the satellite

took more than 10 s to leave the field of view. A simple point-and-shoot strategy was used, without aiming to identify each individual satellite, although the catching of the International Space Station (ISS) was deliberate.

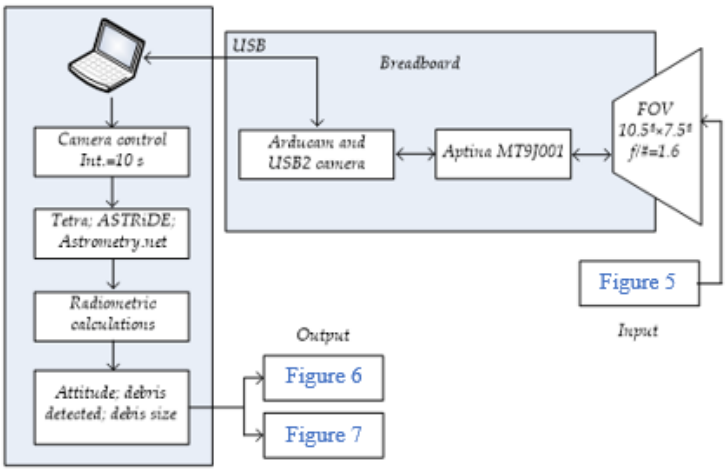

Figure 4. Flow chart of the breadboard operation.

Only four images were selected from the thirteen images collected because they have a possible good number of stars in the field of view, increasing the chances of Tetra extracting the attitude. Two of them are from the ISS, taken with ten seconds difference. The four selected images for testing from ISS are presented in Figure 5.

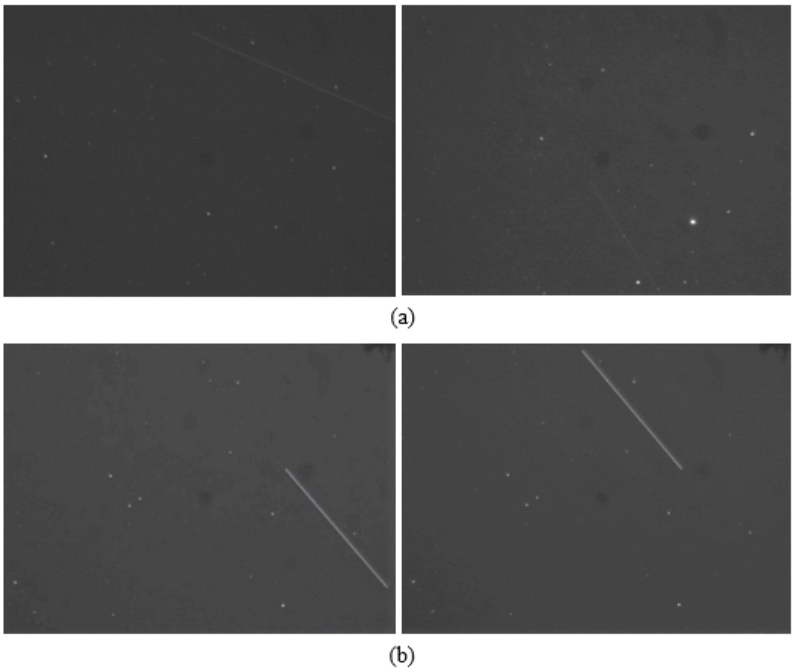

Figure 5. (a) satellite streaks; (b) ISS streaks.

Tetra read the images from Figure 5 to find the attitude. Unfortunately, the algorithm could not determine the position of the images (a), the sky conditions were probably not good enough to extract a reasonable number of stars, the city light pollution at the Observatory was very high, and the Moon was in the sky. Considering Figure 5 images (b), Tetra calculated the attitude for images shown in Figure 6.

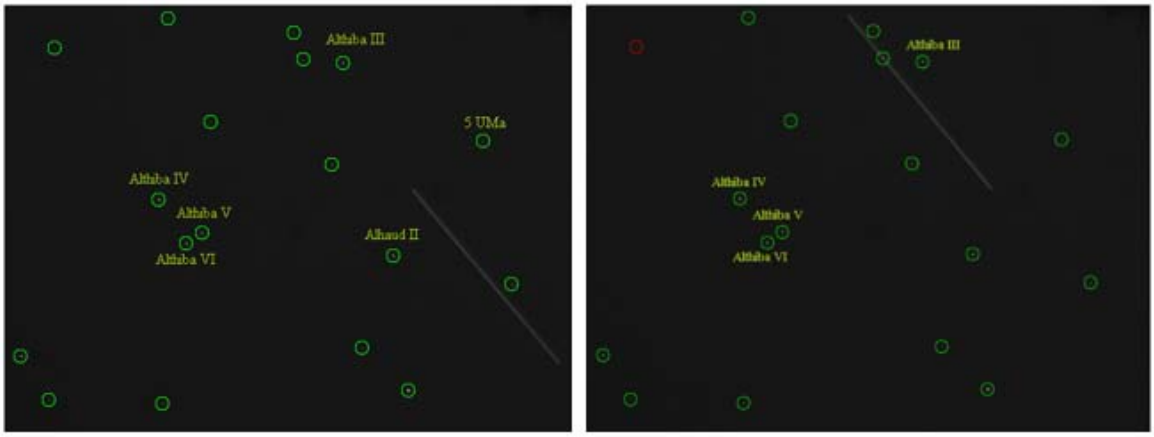

Figure 6. Stars identified by Tetra for images (b) in Figure 5.

In Figure 6, Tetra did not give the names of the stars. The results, i.e., attitude extracted from Tetra and the comparison of the values of right ascension and declination with Astrometry.net, are presented in Table 1.

Table 1. Attitude extracted from Tetra and Astrometry.net

Information	Tetra		Astrometry.net	
	a	b	a	b
Right ascension (deg)	136.3628	136.406	136.374	136.423
Declination (deg)	65.376	65.374	65.375	65.378
Roll (deg)	88.776	88.801	--	--
FOV (deg)	9.905	9.904	--	--
Mismatch probability	$2.074\ 10^{-27}$	$4.86\ 10^{-25}$	--	--

In Table 1, the results from Tetra are in agreement with Astrometry.net proving that the algorithm is reliable in real tests.

After that, all images from Figure 5 were read by ASTRiDE. The ASTRiDE algorithm was able to identify and give information on the streaks of all images, as shown in Figure 7.

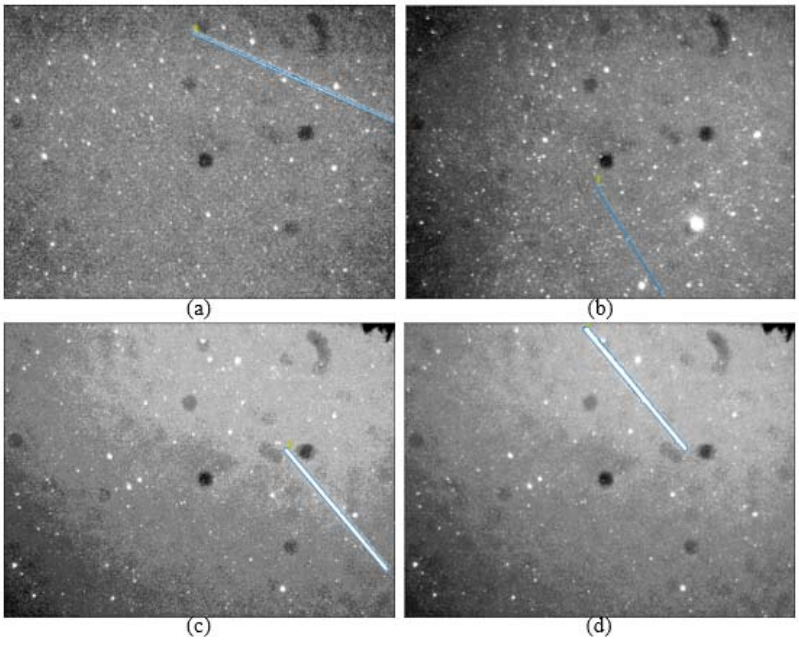

Figure 7. Identified streaks by ASTRiDE.

The streaks results of perimeter and area are presented in Table 2.

Table 2. Streaks results by ASTRIDE

Information (pixel)	Images			
	a	b	c	d
Perimeter	1174.1	568.1	525.1	773.0
Area	1898.9	627.6	1746.6	3670.3

ASTRiDE was also able to identify the streaks in all images, proving to be an appropriate choice for detecting space debris.

- *Case Study_3*

In this case study, the software Image Reduction and Analysis Facility (IRAF) is used to roughly estimate the debris size by photometry on the images. Considering the images in Figure 6, the measurements were done for the indicated stars, of which the magnitudes are known. The stellar fluxes are measured by adding all the digital counts inside a circle centered in the star with a 10-pixel radius. The sky background is calculated by taking an average of the counts on several squares of 25×25 pixels in regions without visible stars. The final flux is converted into magnitudes, and a calibration constant is added to match the cataloged magnitude of each star. The streak's magnitude is measured by taking a rectangle that catches all of its flux and then adding the mean of the calibration constants found for the field stars. Both exposures were of 10 s. The results for debris size estimation are presented in Table 3.

Table 3. Streaks results by ASTRIDE

Star	Catalogued magnitude	Measured image (a)	Calibration constant for image (a)	Measured image (b)	Calibration constant for image (b)
Althiba IV	4.70	20.54	15.84	19.84	15.14
Althiba V	5.15	21.04	15.89	20.31	15.16
Althiba VI	4.80	20.77	15.97	20.02	15.22
Alhaud II	4.65	20.53	15.88	--	--
Althiba III	4.55	20.27	15.72	19.712	15.16
5 UMa	5.70	21.20	15.50	--	--
Average	--	--	15.80	--	15.17
ISS mag	--	--	0.73	--	0.59

Since at the time of observation, in Coimbra, July 15 of 2021, at 22:33 UT, the ISS was at a phase angle ϕ=104 deg, and at a distance to the observer of 997.9 km, it is estimated the diameter, or average cross-section assuming it is a sphere, using (3). Both considering a mix of specular and diffuse contributions and only a diffuse contribution, the results for the ISS size considering the streaks detected was about 20 m in diameter, showing a rather plausible result even with several approximations and without image correction for bias and flatfield corrections, making it possible to estimate an object's size by its streak.

5. Conclusion

This work studied the viability of using a star tracker breadboard to detect space debris in LEO orbits. The breadboard has been built with commercial off-the-shelf components. Tetra algorithm was chosen for the star detection, and ASTRiDE was selected to identify debris.

The system was proven to work. The optical system and the algorithms had good results. Even so, more tests have to be made. Observations with a night sky in better conditions and less light pollution is essential to check if the camera can detect more stars and, thus, verify if Tetra can calculate the attitude for more images. Image reduction for bias and flatfield correction is also essential when aiming at a more precise size estimation of the debris

The algorithms proved themselves to be a good choice. The results of Tetra were very accurate compared to Astrometry.net, and ASTRiDE had the best performance of the tests, detecting all kinds of streaks, even faint ones. Further studies should be done under better night sky conditions and accompanied by bias and flatfield image processing.

Acknowledgment

This research received funding in the framework of the project FLY.PT with references POCI-01-0247-FEDER-046079 and LISBOA-01-0247-FEDER-046079 and with the title Mobilizar a Indústria Aeronáutica Nacional para a Disrupção no Transporte Aéreo Urbano do Futuro (FLY.PT), co-funded for Fundo Europeu de Desenvolvimento Regional (FEDER) of European Union through the Programa Operacional Competitividade and Internacionalização (POCI) of the Programa Operacional Regional de Lisboa 2020, integrated into Portugal 2020. This work was supported by Fundação para a Ciência e a Tecnologia (FCT) through the research grants CENTRA project UIDB/00099/2020; LAETA project UIDB/50022/2020; ICT project UIDP/04683/2020.

References

[1] European Space Agency 2021 *ESA's Annual Space Environment Report* (accessed November 2022) (https://www.sdo.esoc.esa.int/environment_report/Space_Environment_Report_latest.pdf).
[2] ESA's Space Environment Statistics 2021 (accessed November 2022) (https://sdup.esoc.esa.int/discosweb/statistics/).
[3] Pisanu T, Muntoni G, Schirru L, Ortu P, Urru E and Montisci G 2021 *Aerospace* **8(3) 86** 1-10.
[4] Xi J, Xiang Y, Ersoy OK, Cong M, Wei X and Gu J 2020 *IEEE Access* **8** 150864-150877.
[5] ESA 2013 *Space operations-ESA and space debris* (accessed November 2022) (https://www.esa.int/Enabling_Support/Operations/Ground_Systems_Engineering/ESA_Space_Debris_Office).
[6] Klinhrad H 2006 *Space debris-model and risk analysis* Springer: Chichester UK 199-205.
[7] Gordo P, Frederico T, Melicio R, Duzellier S and Amorim A 2020 *Advances in Space Research* **66(2)** 307-320.
[8] Gordo P, Frederico T, Melicio R and Amorim A 2021 *Applied Sciences* **11(3), 948** 1-25.
[9] Duzellier S, Gordo P, Melicio R, Valério D, Millinger M, and Amorim A 2022 *Acta Astronautica* **192** 258-275.
[10] Bonnal C and Darren SMcK 2017 *IAA Situation Report on Space Debris 2016* International Academy of Astronautics: Paris, France.
[11] Fialho MAA and Mortari D 2019 *Sensors* **19(24), 5355** 1-23.
[12] Zakharov AI, Krusanova NL, Moskatiniev IV, Prohorov ME, Stekol'shchikov OY, Sysoev VK, Tuchin MS and Yudin AD 2018 *Solar System Research* **52(7)** 636-643.
[13] Muruganandan VA, Park JH, Maskey A, Jeung I-S, Kim S and Ju G 2016 *Proc. of the 2016 Asia-Pacific International Symposium on Aerospace Technology*, Toyama, Japan, 25-27 October, 1-11.
[14] Christian JA and Crassidis JL 2021 *IEEE Access* **9** 25768-25794.
[15] Vananti A, Schild K and Schildknecht T 2015 *Proc. of Advanced Maui Optical and Space Surveillance Technologies Conference* Maui, Hawaii, USA, 15-18 September, 1-5.
[16] Clemens S 2019 *On-orbit resident space object (RSO) detection using commercial grade star trackers* Master Thesis York University, Toronto, Canada.
[17] Tetra (accessed November 2022) (https://github.com/brownj4/Tetra).
[18] Hipparcos (accessed November 2022) (https://www.cosmos.esa.int/web/hipparcos).
[19] Kim D-W 2016 *ASTRiDE: automated streak detection for astronomical images* (accessed November 2022) (https://github.com/dwkim78/ASTRiDE).